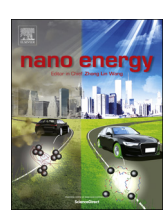
FISEVIER

Contents lists available at ScienceDirect

Nano Energy

journal homepage: www.elsevier.com/locate/nanoen



Full paper

Decoupling the charge collecting and screening effects in piezotronicsregulated photoelectrochemical systems by using graphene as the charge collector



Xiaobo Chen^{a,b}, Lazarus German^a, Jihye Bong^c, Yanhao Yu^a, Matthew Starr^a, Yong Qin^b, Zhenqiang Ma^c, Xudong Wang^{a,*}

- ^a Department of Materials Science and Engineering, University of Wisconsin-Madison, Madison, WI 53706, USA
- ^b Institute of Nanoscience and Nanotechnology, School of Physical Science and Technology, Lanzhou University, Lanzhou 730000, China
- ^c Department of Electrical and Computer Engineering, University of Wisconsin-Madison, Madison, WI 53706, USA

ARTICLE INFO

Keywords: Piezotronics Photoelectrochemistry Water splitting Ferroelectric Graphene

ABSTRACT

Piezotronics have shown great promises in promoting the efficiency of photoelectrochemical (PEC) reactions, while their full-gear functionalities are constrained by the longstanding contradiction between the charge collection of semiconductors and the screening effect of polarization materials. In this report, we tackle this issue by decoupling the collecting and screening trajectories using graphene as the charge collector. The moderate charge density of graphene ensures minimal screen of the adjacent electrical polarizations and concurrently delivers photogenerated free carriers toward the counter electrode. Based on a PMN-PT/graphene/TiO₂ piezotronic PEC system, substantial performance gains were received through tuning the interfacial electronic energy level via ferroelectric polarizations. Forward poling could lead to a 50% improvement of photocurrent density at 1 V vs. RHE and a favorably shifted onset potential. Both calculation and experimental results suggest this outcome was beneficial from the low screening effect from graphene. In contrast, gold electrode will fully screen the polarization from PMN-PT and yield similar PEC performance despite of the poling conditions. This work reveals graphene could be an ideal conductive electrode selection for freeing piezotronic PEC devices from the performance capstone imposed by the trade-off between carrier collecting and charge screening.

1. Introduction

Photoelectrochemical (PEC) reaction is a promising pathway for the direct transformation of solar energy to chemical fuels [1-5]. The past decade has witnessed the prosperity of many PEC conversions in research society, especially the PEC water splitting for H2 generation [6-10]. Nevertheless, the ultimate industry-level solar to hydrogen production through photoelectrochemistry is remained unreachable due to the electrode materials challenges of stability, light absorption and charge separation [11]. Certain strategies (e.g., surface protection, doping, and nanostructure designs) have been developed to tackle these challenges [12-15], while their tunability are approaching the limits due to the restriction of chemistry and material feasibility. In the regard of charge separation, piezotronic effect has arisen as a new paradigm to break the forgoing capstone. The key feature of piezotronics is the interaction between the permanent electrical polarizations and internal electric field formed at the heterojunction interfaces (i.e., the semiconductor/liquid junction for the PEC case) [16-20]. The permanent polarizations are typically produced by intrinsic or strain-induced ionic displacement, corresponding to the ferroelectric and piezoelectric effects, respectively. When a ferroelectric or piezoelectric material presents in a heterojunction, its electrical polarizations would trigger considerable free carrier redistribution in the adjacent semiconductor and thereafter adjust the width and magnitude of the interfacial depletion region. As a result, the charge separation and overall PEC performance can be effectively tuned.

This operational mechanism of piezotronic-modulated PEC reaction implements one fundamental contradiction between the screening effect of permanent polarization and the free charge collection of PEC reactions. The high concentration of free charge in charge collector would inevitably screen the electrical polarization and thus jeopardize the piezotronic tuning effectiveness [19–21]. For high quality piezo- or ferroelectric component, its insulating nature will largely raise the resistance loss of the photogenerated charges [21,22]. One intuitive way to resolve this trade-off is to avoid the passing of free charges through the piezo-/ferroelectric material by inserting a dedicated charge

E-mail address: xudong@engr.wisc.edu (X. Wang).

^{*} Corresponding author.

collector between the semiconductor and the piezo-/ferroelectric material. In this way, highly dielectric piezo-/ferroelectric materials could be used without hindering the overall charge collection. However, most common current collectors (e.g., metals and conductive oxides) have a large density of free electrons and can easily terminate the field effect, meaning the polarization cannot reach the photoactive semiconductor to deliver any band tuning performance. In principle, this challenge can be mitigated if one can use a charge collector that possesses moderate free electron density to balance the charge collecting and screening effects.

Driven by this rationale, herein, we report an implementation of single-layered graphene as the charge collector for disentangling the charge collecting and screening effects in piezotronics-regulated PEC systems. The intermediate free electron density of graphene sitting between metals and semiconductors made it ideal for efficiently scavenging free carriers while imposed minimized influence on the vicinal permanent electrical polarization [23,24]. The graphene piezotronic PEC system was fabricated by sandwiching graphene between a commercial TiO2 P25 powder film and a single crystalline ferroelectric lead magnesium niobate-lead titanate (PMN-PT) slab. Calculation results show that the ferroelectric field from PMN-PT can penetrate through graphene and further alter the energy level of photoactive TiO2. Experimentally, both the photocurrent density and onset potential of TiO₂ electrodes were significantly manipulated by controlling the polarization condition of PMN-PT. This research presented a promising strategy for implementing strong piezotronic enhancement in PEC systems.

2. Experimental section

2.1. Preparation and transferring of graphene

2.1.1. Growth of graphene

Single-layered graphene was grown by chemical vapor deposition (CVD) on a copper substrate following the method reported in previous literature [25]. In the growth, a Cu foil was placed in the CVD tube, which was pumped to $\sim 10\, mTorr$ under a constant H_2 flow of 8.3 sccm. The CVD chamber was maintained at $1010\,^{\circ}C$ for $30\, min$, and then a 50 sccm flow of CH4 was introduced to the chamber. The growth condition was kept for 25 min and a single-layered graphene was deposited on the Cu foil. The CVD system was then cooled down to room temperature naturally under H_2 flow.

2.1.2. PMN-PT substrate preparation

The supporting PMN-PT slap was obtained from TRS Technology Inc. and H.C. Materials Co, without any pre-poling. The films were 1 mm in thickness. Before using, the PMN-PT was polished to reach a surface roughness of $<0.1\,\mu m$. The thickness change after polishing was negligibly small compared to the overall thickness and therefore the final PMN-PT slab was still treated as 1 mm in thickness. Then the PMN-PT surface was treated by oxygen plasma (O₂ 50 sccm, 50 mTorr, 30 W) for 1 min to change its surface to hydrophilic and rinsed by deionized (DI) water for graphene transfer.

2.1.3. Graphene transfer

A layer of polymethyl methacrylate (PMMA) was spin-coated onto the as-received graphene/Cu sample for protection. The Cu foil was then etched using $0.25\,\mathrm{M}$ FeCl $_3$ and 1:10 HF to release the PMMA/graphene layer for transfer. After rinsed with DI water, the floating PMMA/graphene was transferred to the PMN-PT slab and then the PMMA was removed using acetone. For better coverage, another layer of graphene was further transferred onto the PMN-PT through the same procedure.

2.2. Device preparation and fabrication

P25 TiO₂ sample was acquired from Sigma-Aldrich. The TiO₂ paste was prepared by dispersing P25 TiO2 in ethanol solution with a concentration of 0.1 g/ml. Titanium(IV) isopropoxide (TTIP) was then added into the paste as a binding agent during stirring. The suspension was further magnetically stirred for two hours before using. The TiO₂ paste was drop coated onto the graphene/PMN-PT substrate to form a TiO₂ film and was annealed at 200 °C for 2 h in air. A small portion of the graphene surface was uncovered for electrical connection. The TiO₂/graphene/PMN-PT device was then placed in a home-built Atomic Layer Deposition (ALD) system for TiO₂ overcoating. Briefly, the ALD chamber was firstly heated to 120 °C and then TiCl4 and H2O vapor precursors were pulsed into the chamber sequentially with a pulsing time of 0.5 s. The two precursor pulses were separated by 60 s of N2 purging. The detailed methods can be found in our previous works [26,27]. 120 cycles of ALD was applied to grow a 10 nm amorphous TiO₂ coating on the TiO₂ film. A copper film electrode was attached to the back side of the PMN-PT slab for device poling. An electric wire was attached to the exposed graphene surface using silver paste for PEC charge transfer. The entire PMN-PT/graphene/TiO2 system was packaged by epoxy raisin, only leaving a small exposed area for PEC testing. When poling was needed, the PMN-PT slab was poled by directly applying a chosen voltage between the graphene electrode and copper electrode in air for 1 h.

2.3. Characterization and photoelectrochemical (PEC) measurement

Scanning electron microscopy (SEM) images were obtained using a Zeiss LEO 1530 field emission microscope. X-ray diffraction patterns were acquired from a Bruker D8 Discovery with Cu Ku radiation. The PEC measurements were carried out using a three-electrode electrochemical cell with the TiO₂/Graphene/PMN-PT as the working electrode, a Pt wire as the counter electrode, and a saturated calomel electrode (SCE) as the reference electrode. 1 M NaOH was used as the electrolyte. During the measurement, working electrodes were illuminated under a 150 W Xenon lamp with a light intensity of 150 mW/cm². The results were recorded using an Autolab PGSTAT302N station.

3. Results and discussions

The piezotronic PEC system was designed using the permanent polarization from a ferroelectric PMN-PT slab. As schematically shown in Fig. 1a, a graphene layer is placed between the photoanode material (TiO₂) and the PMN-PT slab. Upon illumination, electron-hole pairs are generated in TiO2. Driven by the built-in potential, holes move toward the TiO₂/electrolyte interface and oxidize water into oxygen. Electrons are collected by the graphene layer and driven to the counter electrode for hydrogen production. When the PMN-PT is forwardly biased (defined as positive on the ferroelectric/graphene interface), the ferroelectric polarization will drive electrons toward the interface to balance the charge. Due to the low charge density in graphene, majority electrons need to come from the TiO2 side. Accumulation of electrons can extend the depletion region in the TiO2 side and thus provide extra driving force to facilitate the photo-generated charge separation. Therefore, higher photocurrent can be expected. This design takes the advantage of the unique high conductivity but low charge carrier density feature of graphene. Thus it allows photocurrent to be effectively collected but the ferroelectric polarization can still penetrate deeply into the photoactive material to modulate its electron energy

To test this hypothesis, the interfacial energy level was first calculated using our Mathematica code by incorporating standard materials parameters (calculation details are included in the Supplementary material) [21,22,28]. Fig. 1b is the calculated electron potential distribution at the PMN-PT/graphene/TiO₂ interface under a constant

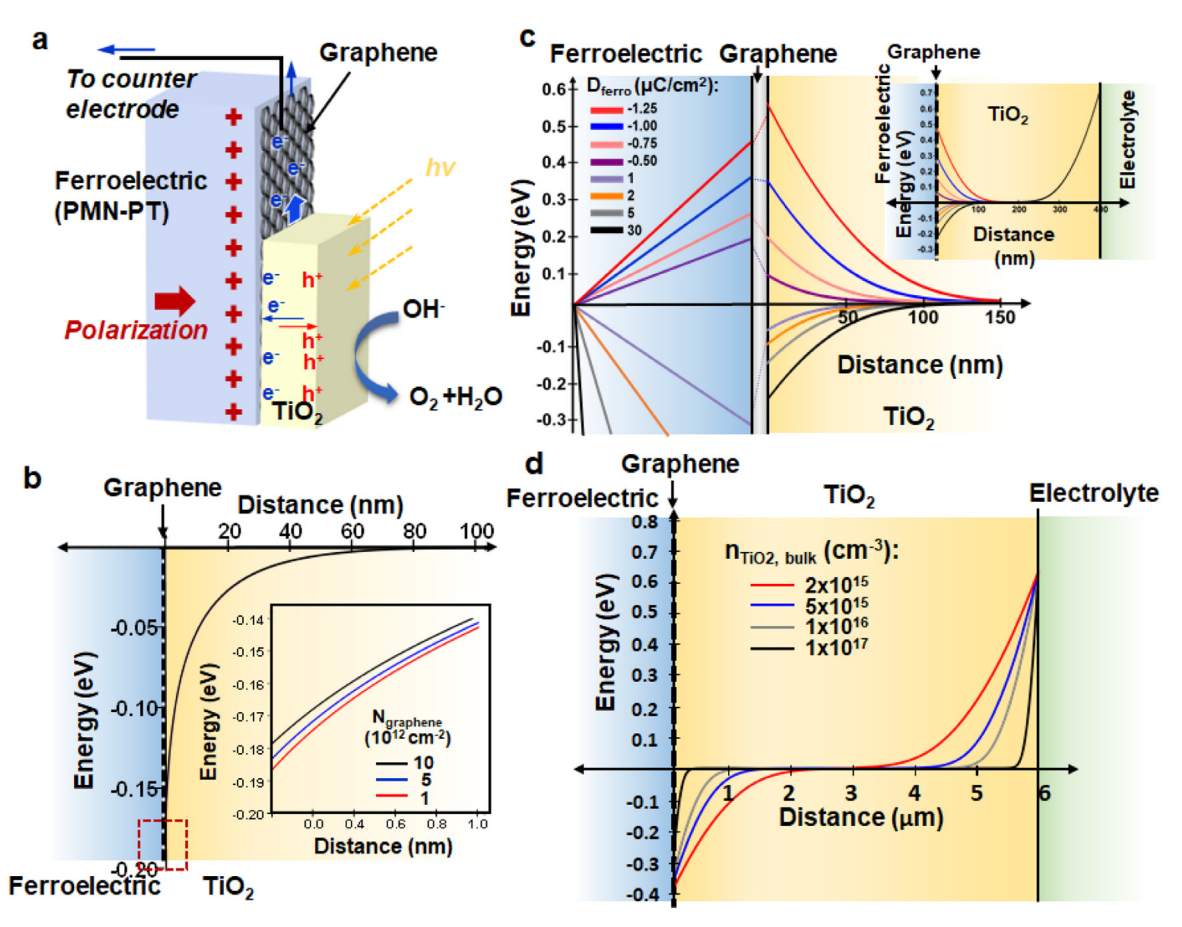


Fig. 1. Piezotronics-modulated interfacial energy level when graphene was used as the charge collector. (a) Schematic diagram of the PMN-PT/graphene/TiO₂ structure showing the function of each component. (b) Calculated interfacial electronic energy level when the graphene layer was assumed to have a charge density of $1-10 \times 10^{12}$ cm² and the ferroelectric polarization was remained a constant $15 \,\mu\text{C/cm}^2$, showing the negligible influences of the graphene charge density to the energy level shifting in the TiO₂ film. (c) Calculated interfacial electronic energy level when the ferroelectric film was poled to different polarization. The thickness of the graphene layer was exaggerated to show the energy level shift due to limited number of free charge inside graphene. Inset is the corresponding full range electronic energy level across the TiO₂ film, showing the ferroelectric polarization only influences the energy level shifting at the PMN-PT/TiO₂ interface, but has negligible influences to the TiO₂/electrolyte interface. (d) Calculated full range electronic energy level across the TiO₂ film at different free carrier concentrations. The ferroelectric polarity was kept at $30 \,\mu\text{C/cm}^2$.

positive ferroelectric polarization of 15 μC/cm². This value is a moderate number that a quality PMN-PT film can normally produce. The charge density of graphene was varied from 10^{12} to 10^{13} cm⁻², which is a normal range of a high quality single-layer graphene [29]. The far end of the PMN-PT slab was set as zero potential point, which was not shown in the plot. The PMN-PT was assumed to be an ideal insulator, i.e. it contributed zero free charge to the interface. The carrier concentration in TiO2 was assumed to be on the order of 1017 cm-3 [30,31]. The plot clearly showed that the graphene charge density within the modeling range exhibited negligible impacts to the energy level in TiO2. All the curves showed a very close depletion depth of ~80 nm. The enlarged interface area revealed the difference in barrier height was less than 0.01 eV when the charge carrier density in graphene changed from 10^{12} to $10^{13}\ cm^{-2}$ (inset of Fig. 1b). This calculation confirmed that a graphene layer can largely preserve the polarization-induced interfacial energy level change in the semiconductor layer, which is the key for piezotronics.

To show the polarization influence, the PMN-PT/graphene/TiO $_2$ interface energy level was further calculated under different ferroelectric polarization, where the free charge carrier concentration was set to be 10^{12} cm $^{-2}$ (Fig. 1c). The thicknesses of PMN-PT and graphene layer were not set to scale for the convenience of illustration. Due to the assumed zero free charge, the potential profiles in PMN-PT were all linear and its interfacial potential was determined by its dielectric property. A slight potential drop occurred through the graphene layer,

due to the screen effect from its limited number of free charges. Under the polarities from 1 to 30 μC/cm², the electron accumulation region extended from 26 to 72 nm, suggesting an enhanced effect of electron collection at the interface, and thus enhanced PEC efficiency. The electron depletion region change showed a much higher sensitivity as it rose from 26 to $112 \, \text{nm}$ over a small range of polarities (-0.50 to $-1.25 \,\mu\text{C/cm}^2$). This is because TiO₂ is a n-type semiconductor, which can screen positive charges more effectively than screening negative charges. Under negative polarities, the electrons are driven toward the electrolyte interface. Therefore, this is the undesired effect and can jeopardize the PEC efficiency. It is worth of noting that even significant change of the energy level can be expected at the ferroelectric side, the energy level at the electrolyte interface does not show noticeable variation (inset of Fig. 1c). This is because the charge densities required for equilibrium is largely controlled by the difference between the Fermi level of TiO₂ and the Nernst potential of the electrolyte, i.e., perturbations in available free charge (calculated from the response of TiO₂ to the given polarizations) are negligible. Therefore, the piezotronic effect to the PEC performance should be primarily attributed to the modulation of charge separation/collection at the ferroelectric (or piezoelectric) / semiconductor interface. In addition, the depletion region is also sensitive to the free carrier concentration in TiO2. As the free electron concentration reduced from $10^{17}\ cm^{-3}$ to the level of 10^{15} cm⁻³, the depletion region significantly expands from 400 nm to nearly 3 μm at a ferroelectric polarity of 30 μC/cm² (Fig. 1d). This situation

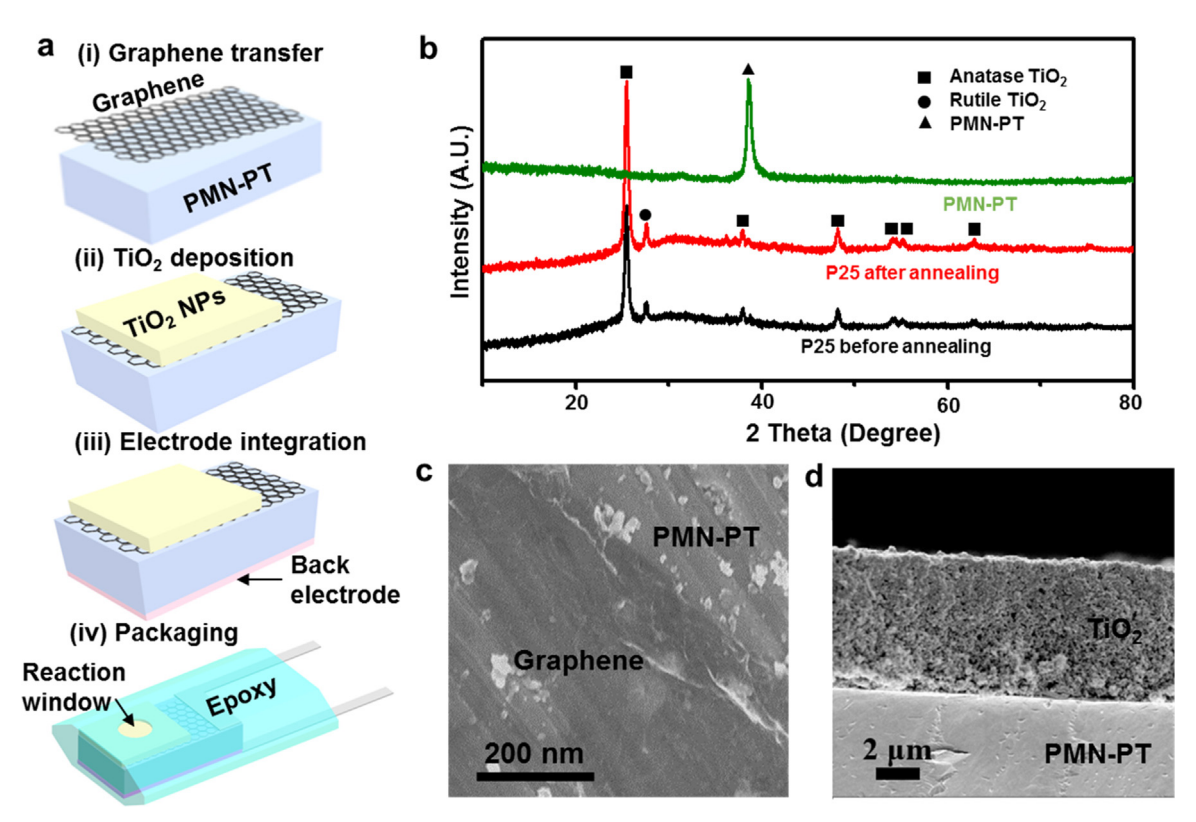


Fig. 2. Ferroelectric-modulated TiO₂ PEC device. (a) Schematic fabrication procedures of a ferroelectric PMN-PT-modulated TiO₂ PEC photoanode, where graphene was applied in-between as the charge collector. (b) XRD spectra of the PEC device at different fabrication stage. (c) A top-view SEM image of the transferred graphene on PMN-PT surface. (d) A cross-sectional SEM image of the PMN-PT/graphene/TiO₂ photoanode.

might more closely represent the case of low-quality ${\rm TiO_2}$ films with a high density of trapping states.

To experimentally test the decoupled effect of charge collection and polarization screening, a piezotronics-regulated PEC system is designed using a ferroelectric PMN-PT slab and a commercial TiO₂ P25 powder photoanode. The schematic fabrication process is shown in Fig. 2a. First, a single-layer graphene was transferred to a PMN-PT slab providing a complete coverage of the PMN-PT surface. After graphene transfer, a layer of TiO_2 nanoparticle film with a thickness of $\sim 6 \, \mu m$ was applied to the graphene surface. The majority graphene surface was covered by TiO2, while only a small top portion was exposed for electrical connection. Then, a copper electrode was applied onto the backside of the PMN-PT slab. A designed electric field was applied between the copper and graphene electrodes to pole the PMN-PT. Finally, the entire device was packaged by epoxy resin leaving a $\sim 9 \text{ mm}^2$ window open for PEC reaction. Fig. 2b shows the x-ray diffraction (XRD) pattern of PMN-PT slab before and after TiO2 layer coating. The PMN-PT slab was oriented along the [111] direction. After TiO₂ coating, the peak from PMN-PT was not observable, while both the anatase and rutile TiO2 phases could be identified. After annealed at 200 °C for 2 h, the crystallinity was significantly enhanced as shown by the stronger (002) diffraction peak, while both anatase and rutile phases were still preserved. The mixed phase was expected to be beneficial to the PEC performance of TiO2 photoanode [32]. The attachment of graphene on PMN-PT was fairly uniform under SEM (darker contrast region in Fig. 2c). The TiO2 film exhibited a coherent contact with the graphene surface without observable discontinuity or significant vacant spots at the interface (Fig. 2d). The entire TiO₂ film was tightly compacted and the thickness was uniform across the entire film.

The PEC performance was then characterized to investigate the ferroelectric polarization influence. Fig. 3a shows the photocurrent density measured from the piezotronic-PEC system before and after the PMN-PT slab was poled under an electric field of 2000 V cm $^{-1}$ for 1 h.

When the PMN-PT slab was not poled, the obtained photocurrent density exhibited a regular bias relationship (black curve in Fig. 3a) and the photocurrent density was 0.08 mA cm⁻² at a bias of 1.0 V versus RHE. This relatively low photocurrent density was typical for the commercial P25 TiO₂ powders due to their poor electric conductivity [27,33]. Although the P25 TiO₂ powders were not idea in PEC photoanode design, they did offer a large room for performance improvement, which is ideal for investigating the piezotronic effect. When the PMN-PT film was poled by a positive electric field of 2000 V cm⁻¹, the corresponding J-V curve exhibited an obvious overall enhancement. The photocurrent density at 1.0 V vs. RHE was found to be 0.12 mA cm⁻², which was 50% enhancement compared to the untreated ones. The open circuit voltage also increased from 0.2 to 0.1 V vs. RHE. When the positively-poled PMN-PT slab was poled oppositely by a $-2000 \,\mathrm{V \, cm}^{-1}$ electric field, the device exhibited an overall decreased current and a higher open circuit voltage (red curve in Fig. 3a). At 1.0 V vs. RHE, the current decreased from 0.08 mA cm⁻² to $0.06\,\text{mA}\,\text{cm}^{-2}$ and the open circuit voltage increased from $0.2\,\text{V}$ to 0.3 V. The J-V curve also exhibited a lower fill factor, suggesting a higher internal resistant. The good accordance of the J-V curves following the poling direction also confirmed the piezotronic regulation is completely reversible.

The piezotronic modulation effect was highly repeatable. From another device that offered a slightly higher original PEC performance, the PMN-PT slab was poled by an electrical field of $\pm~5000\,\mathrm{V\,cm}^{-1}$. As shown in Fig. 3b, at 1.0 V vs REH, the photocurrent density from the forward biased PMN-PT PEC system increased from 0.12 mA cm $^{-2}$ to 0.17 mA cm $^{-2}$, and the open circuit voltage decreased from 0.07 V to 0 V. Similarly, reversely biased PMN-PT showed a significantly lower photocurrent density, which was 0.08 mA cm $^{-2}$ at 1.0 V vs. REH. Accordingly, the open circuit voltage increased to 0.1 V. These photocurrent density changes were the largest enhancement ratio ever being observed from piezotronic modulated systems. Such a strong

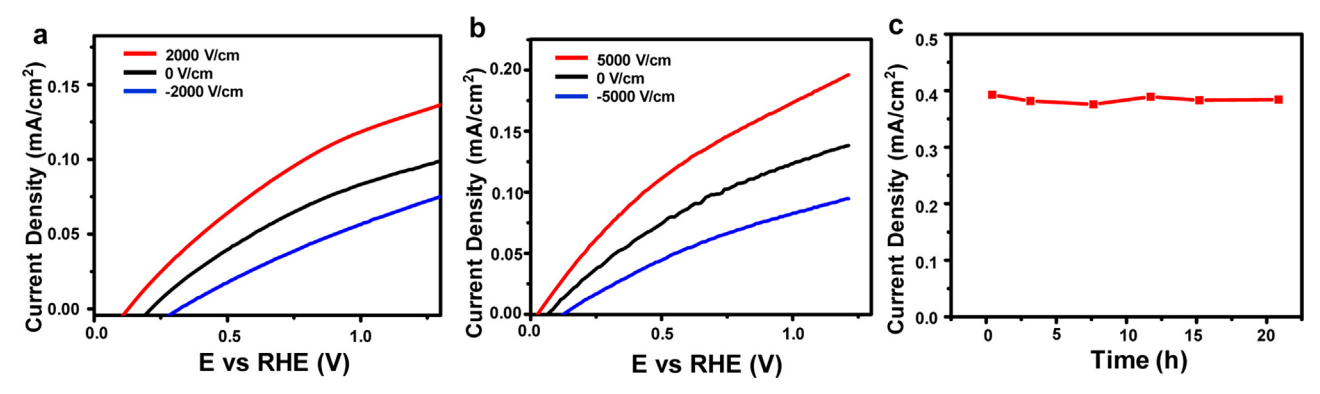


Fig. 3. PEC performance under the influence of ferroelectric polarization. (a) J-V curves of the TiO_2 PEC photoanode when the underlining PMN-PT film was poled by $\pm 2000 \, \text{V cm}^{-1}$ bias. (b) J-V curves the TiO_2 PEC photoanode when the underlining PMN-PT film was poled by $\pm 5000 \, \text{V cm}^{-1}$ bias. (c) Stability test of ferroelectric polarization-enhanced PEC performance.

piezotronic effect could be attribute to two reasons that associated with the utilization of graphene charge collector. First, because of the presence of graphene, PMN-PT did not need to participate in charge collection and transport, therefore it could remain insulating during PEC operation. Second, the PMN-PT slab did not interact with light, therefore it had a minimal photo-generated charges during PEC operation. Both reasons ensured a minimal free charges density in PMN-PT, therefore it could offer an electrical polarization as strong as possible at the TiO₂ interface, even under a high intensity photon illumination. Importantly, this polarization would not be diminished due to the presence of the graphene charge collection layer.

The trend of photocurrent changes under the influence of ferroelectric polarization agreed well with the electronic energy level calculation presented in Fig. 1. As discussed in the calculation section, the photocurrent change was primarily a result of the electron accumulation region change at the PMN-PT/TiO2 interface. Higher polarization generated deeper accumulation region extension and thus larger photocurrent enhancement. Concurrently, the polarization-induced band bending of TiO2 at PMN-PT/TiO2 interface was responsible for the change of open circuit voltage. The downward bending of TiO2 at the PMN-PT/TiO2 interface under forward polarization condition provided extra built-in potential for the electrode and therefore reduced the onset potential. Oppositely, the upward bending of TiO₂ at the PMN-PT/TiO₂ interface under backward polarization condition partially compensated the built-in potential formed at the TiO₂/electrolyte interface and thus increased the onset potential. The 0.1-0.2 eV energy level change of TiO₂ at PMN-PT/TiO₂ interface (inset of Fig. 1c) matched well with the variation of open circuit voltage (~ 0.1 V, Fig. 3a).

An important merit of piezotronic modulation is the interface energy level change could be maintained constantly as long as the polarization holds. To validate this feature, the stability of the photocurrent enhancement was measured as a function of time. A PMN-PT/ graphene PEC device with a relatively high performance was tested. Before the measurement, the device was poled positively under an electric field of 4000 V cm⁻¹ for one hours to ensure a significantly enhanced photocurrent. As shown in Fig. 3c, the nearly 50% photocurrent enhancement was obtained at 1.0 V vs. REH. Then the photocurrent between the graphene electrode and Pt counter electrode was monitored at a constant bias of 1.0 V vs. REH. A high photocurrent of 0.4 mA cm⁻² was maintained for over 20 h without observable decay (Fig. 3d). This long-term stable enhancement confirmed the piezotronic modulation is a long-standing effect and can be used as an effective strategy to improve the PEC performance. In addition, this stable photocurrent enhancement also evidenced the excellent stability of graphene charge collector under corrosive PEC environment.

Our theoretical analysis suggested that the limited free charge carrier density is the key to perform photo-generated charge collection without obvious screening effect to the permanent polarization. To

further demonstrate the merit of graphene electrode, a similar piezotronic-PEC device was fabricated using a thin film of gold as the charge collector instead of graphene. In this device, the thickness of the gold layer on PMN-PT surface was fabricated by thermal evaporation, while the $\rm TiO_2$ layer was remained to be 6 μm prepared by the same approach. Energy level calculations showed that due to the large free charge carrier concentration (5.90 \times 10^{22} cm $^{-3}$) [34], all the charge accumulation and depletion were concentrated at the PMN-PT/Au interface in response to the ferroelectric polarization. As a result, the depletion region in the $\rm TiO_2$ was only influenced by the Fermi level of Au but not responsive to the amplitude and direction of the ferroelectric polarization (Fig. 4a). For a 5-nm Au film, for example, the available current density was 3 orders of magnitude larger than that needed to screen the maximum remnant polarization of the PMN-PT and that needed to

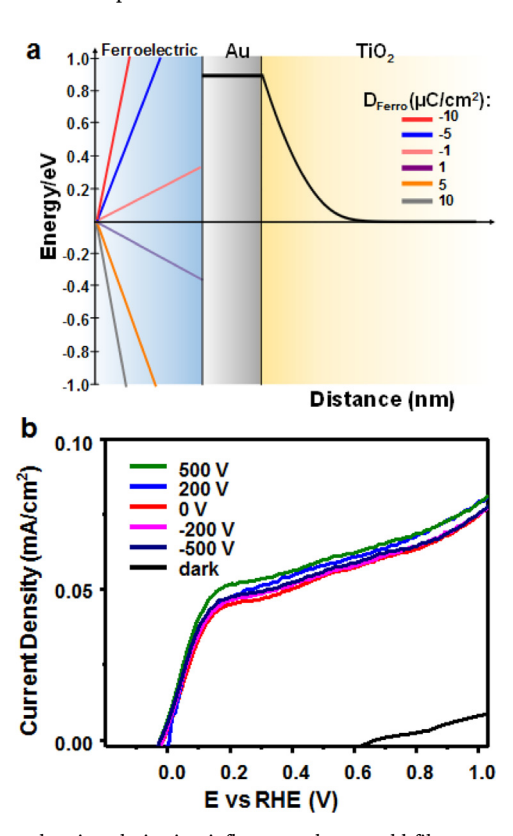


Fig. 4. Ferroelectric polarization influences when a gold film was used as the charge collector. (a) Calculated interfacial electronic energy level when a gold thin film was inserted between the ${\rm TiO_2}$ photoanode and ferroelectric film. (b) J-V curves of the ${\rm TiO_2}$ PEC photoanode when the underlining PMN-PT film was poled by different electrical biases.

bring Au and TiO_2 into equilibrium. Note that Au is able to keep a continuous potential profile by screening the PMN-PT on an Å scale which is why there appears potential step at PMN-PT/Au interface.

This is the situation of complete screening and no piezotronic modulation can be expected. Experimental measurement revealed the PEC behavior as expected. As shown in Fig. 4b, five J-V curves were measured for the PMN-PT/Au/TiO2 system for unpoled PMN-PT and after the PMN-PT slab was poled under electrical fields of $-2000,\ 2000,\ -5000,\$ and $5000\$ V cm $^{-1}.$ All the curves exhibited a very similar shape and no significant difference in either photocurrent density and open circuit voltage can be observed. This comparison confirmed the importance of charge collector selection and the unique role of graphene in preserving the electrical polarization while carrying the photo-generated charges.

4. Conclusion

In this work, single-layered graphene was used as the charge collector in between a ferroelectric PMN-PT slab and photoactive TiO₂ film. Numerical calculation showed that due to the limited free charge carrier density, the electrical polarization generated in the ferroelectric layers can effectively tune the electronic energy level in the semiconducting TiO₂ film. Meanwhile, the high charge mobility of graphene still allowed rapid transport of photogenerated charges to the counter electrode. Experimental results well agreed with this calculation prediction. Up to 50% photocurrent enhancement was obtained from positively poled PMN-PT slab. This is by far the largest improvement ratio based on piezotronic modulation, as a result of the effective decoupling of polarization generation and charge transport. The unique role of graphene in this decoupling effect was further supported by replacing it with a gold thin film. This research provided an effective solution to one of the key challenges of piezotronics-regulated PEC systems, where effective charge collection requires high conductivity but a maximal ferroelectric/piezoelectric polarization require the material to be insulating. Although this study was done on a ferroelectric material, the same principle can be broadly applied to general strained piezoelectric materials enabling maximum piezotronics enhancement in electrochemical systems for efficient power generation and storage.

Acknowledgement

This work was supported by the National Science Foundation under Award Nos. DMR-1709025 and CMMI-1148919. X.C. thanks the support of China Scholarship Council.

Appendix A. Supplementary material

Supplementary data associated with this article can be found in the

online version at http://dx.doi.org/10.1016/j.nanoen.2018.03.066.

References

- [1] M. Gratzel, Nature 414 (2001) 338-344.
- [2] M.G. Walter, E.L. Warren, J.R. McKone, S.W. Boettcher, Q.X. Mi, E.A. Santori, N.S. Lewis, Chem. Rev. 110 (2010) 6446–6473.
- [3] A. Mills, S. LeHunte, J. Photochem. Photobiol. A-Chem. 108 (1997) 1-35.
- [4] M.S. Dresselhaus, I.L. Thomas, Nature 414 (2001) 332-337.
- [5] O. Khaselev, J.A. Turner, Science 280 (1998) 425-427.
- [6] Y. Yu, Z. Zhang, X. Yin, A. Kvit, Q. Liao, Z. Kang, X. Yan, Y. Zhang, X. Wang, Nat. Energy 2 (2017) 17045.
- [7] M.J. Kenney, M. Gong, Y. Li, J.Z. Wu, J. Feng, M. Lanza, H. Dai, Science 342 (2013) 836–840.
- [8] F. Lin, S.W. Boettcher, Nat. Mater. 13 (2014) 81-86.
- [9] J.C. Hill, A.T. Landers, J.A. Switzer, Nat. Mater. 14 (2015) 1150-1155.
- [10] O. Khaselev, Science 280 (1998) 425-427.
- [11] N.S. Lewis, Science 351 (2016) aad1920.
- [12] Y.W. Chen, J.D. Prange, S. Duhnen, Y. Park, M. Gunji, C.E. Chidsey, P.C. McIntyre, Nat. Mater. 10 (2011) 539–544.
- [13] T.W. Kim, K.S. Choi, Science 343 (2014) 990-994.
- [14] S. Hu, M.R. Shaner, J.A. Beardslee, M. Lichterman, B.S. Brunschwig, N.S. Lewis, Science 344 (2014) 1005–1009.
- [15] Y. Yu, X. Yin, A. Kvit, X. Wang, Nano Lett. 14 (2014) 2528-2535.
- [16] W. Wu, Z.L. Wang, Nat. Rev. Mater. 1 (2016) 16031.
- [17] Z.L. Wang, Adv. Mater. 24 (2012) 4632–4646.
- [18] Z.L. Wang, Nano Today 5 (2010) 540-552.
- [19] Y. Inoue, M. Okamura, K. Sato, J. Phys. Chem. 89 (1985) 5184-5187.
- [20] Y. Inoue, K. Sato, K. Sato, H. Miyama, J. Phys. Chem. 90 (1986) 2809-2810.
- [21] F. Wu, Y. Yu, H. Yang, L.N. German, Z. Li, J. Chen, W. Yang, L. Huang, W. Shi, L. Wang, X. Wang, Adv. Mater. 29 (2017).
- [22] W.G. Yang, Y.H. Yu, M.B. Starr, X. Yin, Z.D. Li, A. Kvit, S.F. Wang, P. Zhao, X.D. Wang, Nano Lett. 15 (2015) 7574–7580.
- [23] K.S. Novoselov, A.K. Geim, S.V. Morozov, D. Jiang, Y. Zhang, S.V. Dubonos, I.V. Grigorieva, A.A. Firsov, Science 306 (2004) 666–669.
- [24] C. Lee, X. Wei, J.W. Kysar, J. Hone, Science 321 (2008) 385-388.
- [25] D.-W. Park, S.K. Brodnick, J.P. Ness, F. Atry, L. Krugner-Higby, A. Sandberg, S. Mikael, T.J. Richner, J. Novello, H. Kim, D.-H. Baek, J. Bong, S.T. Frye, S. Thongpang, K.I. Swanson, W. Lake, R. Pashaie, J.C. Williams, Z. Ma, Nat. Protoc. 11 (2016) 2201–2222.
- [26] Y. Yu, Z. Li, Y. Wang, S. Gong, X. Wang, Adv. Mater. 27 (2015) 4938-4944.
- [27] Y. Yu, J. Li, D. Geng, J. Wang, L. Zhang, T.L. Andrew, M.S. Arnold, X. Wang, ACS Nano 9 (2015) 564–572.
- [28] H. Li, Y. Yu, M.B. Starr, Z. Li, X. Wang, J. Phys. Chem. Lett. 6 (2015) 3410-3416.
- [29] T. Ohta, A. Bostwick, J.L. McChesney, T. Seyller, K. Horn, E. Rotenberg, Phys. Rev. Lett. 98 (2007) 206802.
- [30] H. Tang, K. Prasad, R. Sanjinès, P.E. Schmid, F. Lévy, J. Appl. Phys. 75 (1994) 2042–2047.
- [31] G.A. Acket, J. Volger, Phys. Lett. 8 (1964) 244-246.
- [32] D.C. Hurum, A.G. Agrios, K.A. Gray, T. Rajh, M.C. Thurnauer, J. Phys. Chem. B 107 (2003) 4545–4549.
- [33] C.H. Kang, L.Q. Jing, T. Guo, H.C. Cui, J. Zhou, H.G. Fu, J. Phys. Chem. C 113 (2009) 1006–1013.
- [34] N.W. Ashcroft, N.D. Mermin, Solid State Physics, Holt, Rinehart and Winston, New York, 1976.